

THE METALLICITY GRADIENT OF THE THICK DISK BASED ON RED HORIZONTAL BRANCH STARS FROM SDSS DR8

Y.Q. CHEN, G. ZHAO, K. CARRELL, & J.K. ZHAO

Draft version August 6, 2018

ABSTRACT

Based on SDSS DR8, we have selected a sample of 1728 red horizontal branch stars with $|Z| < 3$ kpc by using a color-metallicity relation and stellar parameters. The sample stars clearly trace a typical thick disk population with peaks at $|Z| = 1.26$ kpc and $[\text{Fe}/\text{H}] = -0.54$. The vertical metallicity gradient of the thick disk is estimated in two ways. One is a fit to the Gaussian peaks of the metallicity histograms of the thick disk by subtracting minor contributions from the thin disk and the inner halo based on the Besançon Galaxy model. The resulting gradient is -0.12 ± 0.01 dex kpc^{-1} for $0.5 < |Z| < 3$ kpc. The other method is to linearly fit the data based on stars with $1 < |Z| < 3$ kpc being the main component of the thick disk. Five subgroups are then selected in different directions in the $X - |Z|$ plane to investigate the difference in the vertical metallicity gradient between the Galactocenter and anti-Galactocenter directions. We found that a vertical gradient of -0.22 ± 0.07 dex kpc^{-1} is detected for five directions except for one involving the pollution of stars from the bulge. The results indicate that the vertical gradient is dominant, but a radial gradient has a minor contribution for the thick disk population represented by RHB stars with $1 < |Z| < 3$ kpc. The present work strongly suggests the existence of a metallicity gradient in the thick disk, which is thought to be negligible in most previous works in the literature.

Subject headings: Stars:horizontal-branch - Stars:late-type - Galaxy: disk - Galaxy: kinematics and dynamics - Galaxy: structure

1. INTRODUCTION

The presence of the thick disk component in the Galaxy has been established for several decades (Gilmore & Reid 1983). The age, metallicity and rotational velocity of thick disk stars have been investigated for various types of stars in the solar neighborhood. However, the formation mechanism of the thick disk is not well known. Actually, the metallicity gradient for the thick disk, being a basic input for the model of the Galactic disk, is not well studied in the literature. To the contrary, the traditional radial metallicity gradient of the Galactic thin disk is well investigated based on *HII* regions, Cepheids, OB stars, open clusters (young population) and planetary nebulae (old population). It is found that the radial gradients vary with time in the sense of a steeper slope in the early stages compared to the present value, and there is a change in slope at large Galactocentric distances $R > 10$ kpc (Maciel & Costa 2009).

Generally, the thick disk is typical for vertical distances from the Galactic plane of 0.5 to 1.5 kpc based on observational data in the solar neighborhood. With a large spectroscopic survey of stars far away from the Sun, it is suggested that stars with $1 < |Z| < 3$ kpc dominate the thick disk (Allende Prieto et al. 2006), and the edge of the thick disk could reach up to $|Z| \sim 5.5$ kpc. The large range in the $|Z|$ distribution enables us to investigate the vertical metallicity gradient of the thick disk, which is not possible for the thin disk where most stars are located within $|Z| < 0.5$ kpc. Such a study has recently begun and the existence of a metallicity gradi-

ent in the thick disk is a discrepant issue. For example, Allende Prieto et al. (2006) proposed no metallicity gradient in the thick disk for $1 < |Z| < 3$ kpc with an upper limit on the gradient of 0.03 dex kpc^{-1} , while Katz et al. (2011) investigated the metallicity distribution function (hereafter MDF) of the thin-thick-disk-halo system in two Galactic directions for several intervals between 0 and 5 kpc above the Galactic plane and detected a vertical metallicity gradient of -0.068 ± 0.009 dex kpc^{-1} . Siegel et al. (2009) suggested that the thick disk presents no metallicity gradient. But some models with a gradient are compatible with observations of the thick disk dominated by a population with $1 < |Z| < 4$ kpc as pointed out by Katz et al. (2011). Meanwhile, in an indirect way, the mean metallicity for the thick disk varies with different heights from -0.48 ± 0.05 at $0.4 < |Z| < 0.8$ kpc (Soubiran et al. 2003), to -0.685 ± 0.004 and -0.780 at $1 < |Z| < 3$ kpc (Siegel et al. 2009), which may indicate the existence of a metallicity gradient. Note that these works are mainly based on dwarf stars and they have limitations in some aspects. For example, Soubiran et al. (2003) have high resolution but low signal-to-noise data for low heights of $0.4 < |Z| < 0.8$ kpc where both the thin and thick disks contribute significantly to the MDF. Allende Prieto et al. (2006) and Ivezić et al. (2008) were based on an SDSS DR6 sample where metallicity on the metal rich side could be underestimated by 0.2-0.3 dex according to Bond et al. (2010). Siegel et al. (2009) are based on photometrically derived metallicities, which are not as good as spectroscopically derived values. Recently, Katz et al. (2011) provide high quality data for the metallicity estimation, but the number of sample stars is limited to several hundreds.

The aim of this work is to probe the metallicity gra-

Key Laboratory of Optical Astronomy, National Astronomical Observatories, Chinese Academy of Sciences, Beijing, 100012, China; cyq@bao.ac.cn.

dient of the thick disk population using red horizontal branch (hereafter RHB) stars selected from SDSS DR8. This study has some advantages over previous studies. First, the number of stars in the sample is on the order of thousands, and the metallicity is based on the updated version in SDSS DR8. Second, RHB stars are an interesting type of star, which are different from dwarf stars, with stellar distances easily obtained from their intrinsic absolute magnitude. Their high brightness make them traceable to distances of up to 10 kpc. Finally, we investigate the metallicity distributions for thick disk stars in five different directions in the $X - |Z|$ plane. In particular, the comparison of the thick disk properties between the Galactocenter and anti-Galactocenter directions has great potential for providing more stringent data for model comparisons. Thanks to the large survey area of the SDSS project, it is the first time that such properties in different directions can be studied and they will provide important clues for our understanding of the thick disk formation.

2. THE SAMPLE STARS

The selection procedure of RHB stars is similar to Chen et al. (2010), but uses SDSS DR8 (Aihara et al. 2011) rather than SDSS DR7 (Abazajian et al. 2009). Specifically, the first selection criterion is the color-metallicity relation of $(g-r)_0 = 0.343(\pm 0.039)[\text{Fe}/\text{H}] + 0.829$ presented in Chen et al. (2010) with a deviation in $(g-r)_0$ to the above relation $\delta < 0.20 \text{ mag}$. Then stars with $g_0 < 20 \text{ mag}$, $[\text{Fe}/\text{H}] > -2.0$ and signal-to-noise ratios of their spectra larger than 10 are used to obtain good quality data. Thirdly, RHB stars should have stellar parameters within the range of 4500–5900 K in temperature and 1.8–3.5 dex in $\log g$. In the selection, photometric data and stellar parameters (including metallicities) in photometric and spectroscopic STAR tables of DR8 are adopted. Stellar distances of stars are calculated from g magnitudes and the absolute magnitude-metallicity relation of $M_g = 0.492[\text{Fe}/\text{H}] + 1.39$ derived by Chen et al. (2009) with metallicities taken from the SDSS DR8 spectroscopic STAR table. The stellar distance and position on the sky is then converted to the cartesian system of Galactic coordinates (X, Y, Z).

As shown in Aihara et al. (2011), the photometric data and stellar parameters are updated in DR8 along with an enlarged survey area in the disk. Both improvements provide a better chance for us to probe the thick disk properties. With the aim to investigate the properties of the thick disk, the sample stars are selected to have $|Z| < 6$ kpc since the edge of the thick disk is at about 5.5 kpc above the Galactic plane as suggested by Majewski (1994). With this limit, we extract a sample of 2,729 RHB candidate stars from SDSS DR8. The left panel of Fig. 1 shows the distributions of distance to the Sun, vertical distance to the Galactic plane and Galactic latitude of the sample. In particular, the $|Z|$ distribution of RHB stars has a peak around $|Z| = 1.2$ kpc and most of them are located within $|b| = 6 - 16^\circ$ with a weak tail extending to $|b| = 40^\circ$. There is a hint of a minimum in the $|Z|$ distribution at $|Z| = 3$, which is taken as the selection limit of the thick disk in many works. After that, $|Z|$ flattens out from $|Z| = 3$ kpc to $|Z| = 6$ kpc where we cut our sample. As we know that many previous works select thick disk stars with $|Z| < 3$ kpc or $|Z| < 4$ kpc, in

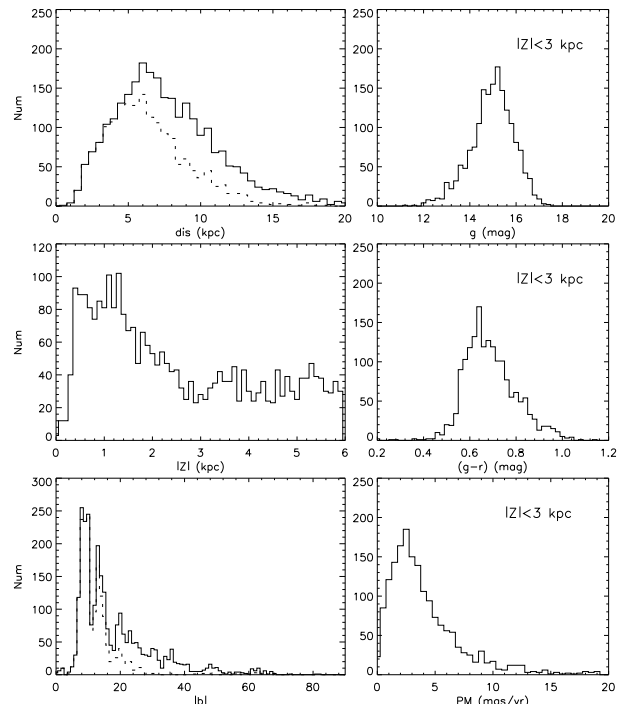


Figure 1. Left: The distributions of distance, $|Z|$ magnitude and galactic latitude for RHB stars with $|Z| < 6$ (the thick line) and $|Z| < 3$ (the dashed line). Right: The g_0 magnitude, $(g-r)_0$ color and proper motion distributions for stars with $|Z| < 3$.

the present work, we limit our sample to $|Z| < 3$ kpc and 1728 RHB stars are selected for studying the metallicity gradient. Most of them are limited to within 10 kpc and $|b| < 20^\circ$ as shown in the dashed lines in the left panel of Fig. 1.

The right panel of Fig. 1 shows the g_0 magnitude, $(g-r)_0$ color and proper motion (PM) distributions of our sample stars. In comparison with the selection criteria for stars in the SDSS/SEGUE survey Yanny et al. (2009), we found the main contribution of our sample stars comes from K (and partly red K) giants, which covers the metallicity range of $[\text{Fe}/\text{H}] \sim -2.0$ to the solar value (with $l^e > 0.07$), has g magnitudes brighter than 18.5 mag, $PM < 11 \text{ mas/yr}$ and a color range of $(g-r)_0 = 0.5$ to 0.8 mag. These criteria will not produce a significant distance or metallicity bias in our sample selection, and thus we assume that these target selections in SDSS/SEGUE will not affect our result.

3. ANALYSIS AND RESULTS

3.1. The metallicity distribution of the thick disk

The metallicity distribution of our sample stars is shown in the upper panel of Fig. 2. It shows that the contribution from the thin disk is significant with 550 stars having $[\text{Fe}/\text{H}] > -0.25$ and a peak at $[\text{Fe}/\text{H}] = -0.12$. The peak at $|Z| = 0.8$ kpc in Fig. 1 partly corresponds to this population. The halo has a negligible contribution with only 77 stars having $[\text{Fe}/\text{H}] < -1.0$. There are 1101 stars with $-1.0 < [\text{Fe}/\text{H}] < -0.25$, corresponding to the thick disk, which have peaks at $|Z| = 1.26$ kpc and $[\text{Fe}/\text{H}] = -0.54$.

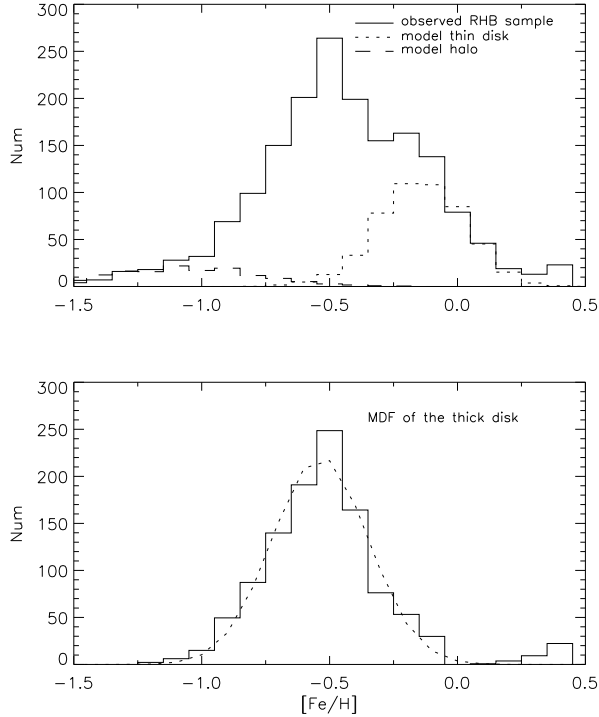


Figure 2. The $[\text{Fe}/\text{H}]$ distribution of the sample stars before and after subtracting the contributions from the model thin disk and halo populations.

In order to exclude the contribution of the thin disk and the halo, we obtain simulation data from the Besançon Galaxy model (Robin et al. 2003) using the selection criteria: (i) $12 < g < 20 \text{ mag}$; (ii) $b = -30^\circ$ to 30° with a step size of 10° ; (iii) $l = 50^\circ$ to 250° with a step size of 25° ; (iv) absolute magnitude $M_V = 0.0 - 1.2$ and spectral type from F to K; (v) population being either thin disk or halo; and (vi) the color-metallicity relation and stellar parameter ranges for selecting RHB stars in Chen et al. (2010). All these criteria fit our observed RHB star sample. Then, the metallicity distributions of the simulated data for the thin disk and halo are normalized to the star numbers in the observed RHB sample for each population respectively. Coincidentally, the simulated thin disk from the model has the same metallicity peak at $[\text{Fe}/\text{H}] = -0.115$ and the simulated halo has negligible contribution to the metallicity distribution as shown by the dashed lines in the upper panel of Fig. 2. The MDF of the thick disk after subtracting the simulated thin disk and halo contributions is shown in the lower panel of Fig. 2. A Gaussian fit to the metallicity histogram is performed and has a peak at $[\text{Fe}/\text{H}] = -0.54$, which is quite close to the peak of the histogram.

3.2. The metallicity gradient of the thick disk

In our sample, there are significant numbers of stars at different $|Z|$ ranges of $0.5 - 1.0 \text{ kpc}$, $1.0 - 1.5 \text{ kpc}$, $1.5 - 2.0 \text{ kpc}$, $2.0 - 2.5 \text{ kpc}$, and $2.5 - 3.0 \text{ kpc}$ in the middle panel of Fig. 1. Thus, it provides a way to investigate the metallicity gradient for $0 < |Z| < 3 \text{ kpc}$. We perform the same procedure to each of the five differ-

Table 1
Thick disk metallicity peak as a function of height

Height kpc	median Z kpc	TD peak	Num
[0.5, 1.0]	0.74	-0.432 ± 0.017	416
[1.0, 1.5]	1.26	-0.480 ± 0.013	443
[1.5, 2.0]	1.74	-0.559 ± 0.017	308
[2.0, 2.5]	2.23	-0.620 ± 0.019	242
[2.5, 3.0]	2.71	-0.651 ± 0.033	159

ent $|Z|$ bins as that in Sect.3.1 and obtain the Gaussian peak of the metallicity histogram for each $|Z|$ bin. Fig. 3 shows the metallicity distribution for the $1.0 < |Z| < 1.5 \text{ kpc}$ bin before and after subtracting contributions from the thin disk and halo components based on model data. The resulting peak metallicities from the Gaussian fits to the metallicity histograms for five different $|Z|$ bins are shown in Table 1, as well as the height range, the median $|Z|$ and the star counts. The bin size for the plotted histograms are 0.05 dex and we have checked that a bin size of either 0.02 or 0.10 will not significantly change the Gaussian peak in the fit, but the distribution will deviate from a Gaussian function for one or two bins. The errors in the metallicity peak in Table 1 are estimated by the Gaussian dispersion of the metallicity peaks from 1000 simulated samples randomly selected from the observed samples for each height bin using a bootstrap method. Fig. 4 shows the peak metallicity of the thick disk MDF as a function of median $|Z|$ and the metallicity gradient is estimated from the weighted least squares fit to the data. The metallicity gradient is $-0.12 \pm 0.01 \text{ dex kpc}^{-1}$ with an intercept of -0.34 dex . This gradient is slightly steeper than that of Katz et al. (2011) who found $-0.068 \pm 0.009 \text{ dex kpc}^{-1}$ with an intercept of -0.46 dex .

In order to estimate the errors from the Besançon Galaxy model, we vary the normalization factors in both the halo and the thin disk components by reducing and enhancing the adopted value by 10%, which is a worst case scenario, and the modeled metallicity distributions deviate clearly from the observed distributions. We therefore obtain an additional four sets of Gaussian metallicity peaks of the thick disk for each bin. In total, we have five sets of metallicity distributions for five $|Z|$ bins, which produces 3125 metallicity gradients in the lower panel of Fig. 4. All these slopes lie within -0.11 to -0.15 , and thus the errors from uncertainties in the Besançon model do not have a significant effect on the metallicity gradients.

3.3. The $[\text{Fe}/\text{H}]$ versus $|Z|$ diagram in five different directions in the $X - |Z|$ plane

Katz et al. (2011) compared the metallicity distributions in two different directions in order to investigate the origin of the gradient from either vertical or radial variations. They found that the vertical origin is strongly favored and the Kolmogorov-Smirnov test (hereafter KS test) shows similar metallicity distributions for two fields directed at M3 and M5 with different $X - Z$ directions. Since both of the two directions in Katz et al. (2011) are located in the anti-Galactocenter direction, it is interesting to make this comparison for different directions, including some Galactocenter directions. Meanwhile, the previous method to estimate the metallicity gradient is

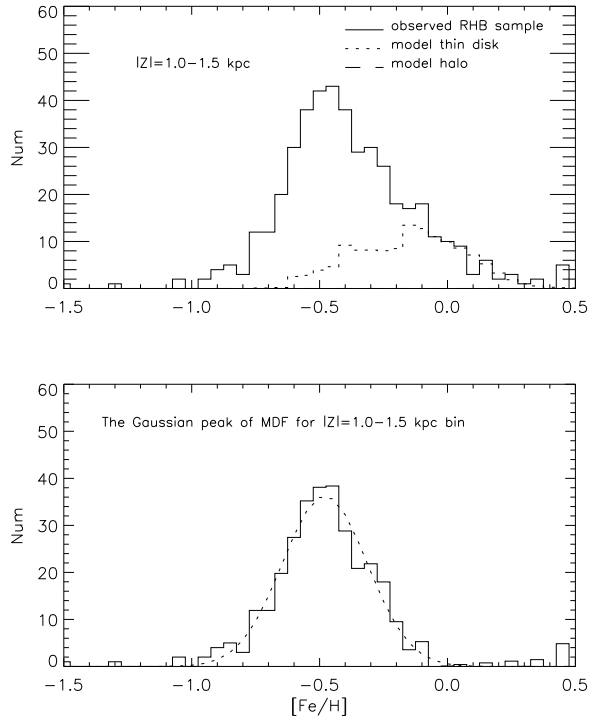


Figure 3. The same as Fig.2 but for the $1.0 < |Z| < 1.5$ bin.

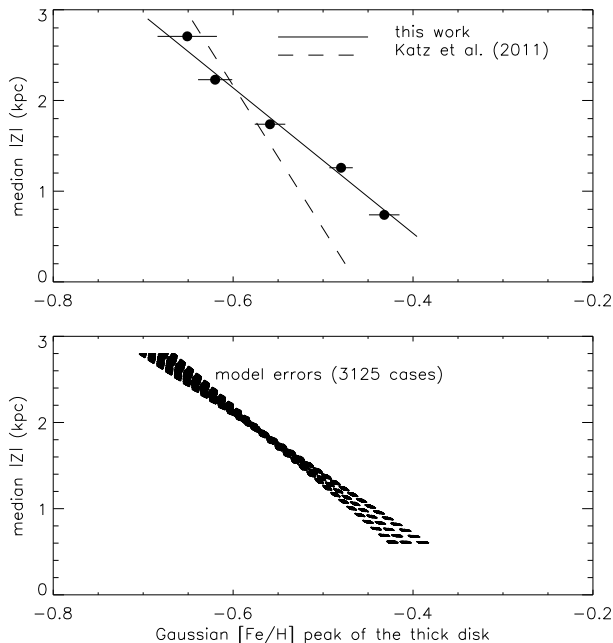


Figure 4. The metallicity gradient for the thick disk for $|Z| = 0-3$ kpc in this work (solid line) as compared with that from Katz et al. (2011) (dashed line).

based on the assumption that the thick disk does not include stars with high metallicity ($[\text{Fe}/\text{H}] \sim -0.12$), which is arbitrarily assigned to be the thin disk popu-

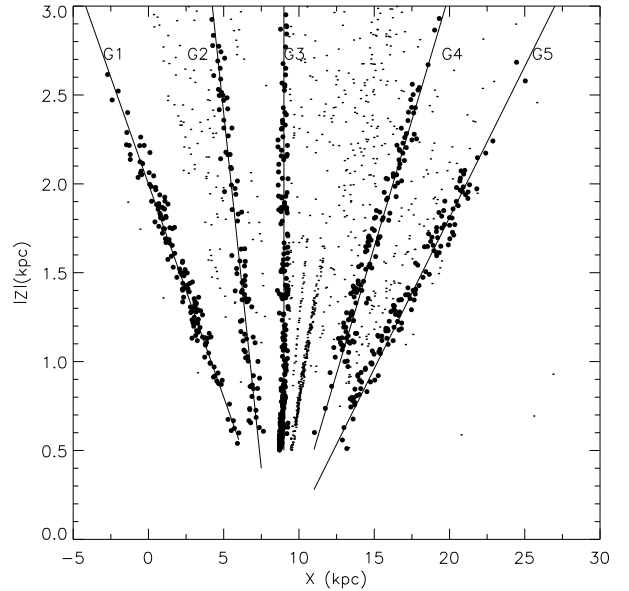


Figure 5. Five star groups, G1 to G5, selected in the $X - |Z|$ plane.

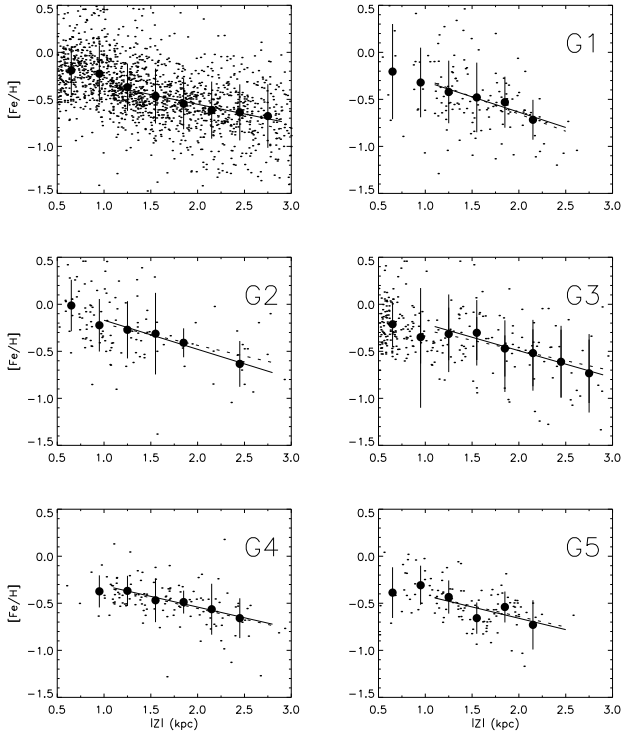
lation, and does not include stars with low metallicity ($[\text{Fe}/\text{H}] < -1.0$), which is arbitrarily assigned to be the halo population. Actually, the thick disk can extend to a metallicity of $[\text{Fe}/\text{H}] = 0.0$ and a metal weak component of the thick disk is widely accepted to exist in the Galaxy. Therefore, we perform an alternative way to trace the metallicity gradient using the $[\text{Fe}/\text{H}]$ versus $|Z|$ diagram, which is used in many works. In particular, it is important to know how the metallicity distributions vary between the Galactocenter and anti-Galactocenter directions since the scale length of the thick disk typically ranges from 2.2 to 3.6 kpc (Morrison et al. 1990; Robin et al. 1996; Carollo et al. 2010). In our sample, it is possible to select stars in five different directions in order to investigate the properties of the thick disk on both sides of the solar circle. Fig. 5 shows the selection of five groups (G1 to G5) of stars in the $X - |Z|$ plane with the G1 and G2 fields toward the Galactic center, G4 and G5 toward the anti-Galactocenter direction, and G3 is limited to the solar region of $X = 8.3$ to 9.3 kpc. Here X is along the line between the Sun and the Galactic center and $|Z|$ is the absolute value of the vertical distance to the Galactic plane.

Fig. 6 shows the $[\text{Fe}/\text{H}] - |Z|$ diagrams for all stars with $0.5 < |Z| < 3.0$ kpc in five directions. Stars with $|Z| < 0.5$ kpc are excluded because they are missing in most directions and large contributions from the thin disk persist. The metallicity gradients are investigated by using mean metallicity at different height bins for five groups of stars. It is clear that all five groups show the existence of a metallicity gradient. A careful inspection of Fig. 6 shows the first two points with $|Z| < 1.0$ kpc are quite different inside the solar circle (G1 and G2) compared to outside the solar circle (G4 and G5). In view of the fact that the thick disk is predominant for $1 < |Z| < 3$ kpc while a star located between 0.5 and 1.0 kpc has equal chances to be in either the thin or thick

Table 2

The metallicity gradient in the formula of $[\text{Fe}/\text{H}] = a|Z| + b$ based on data for the five groups.

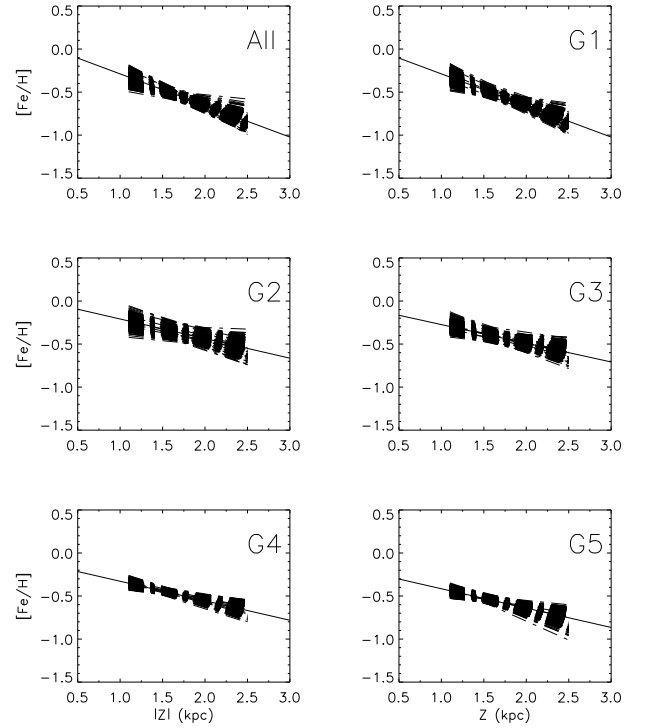
Groups	a (σ_a)	b	scatter	Num
G1	-0.367 ± 0.074	0.078	0.162	140
G2	-0.228 ± 0.069	0.019	0.148	123
G3	-0.217 ± 0.058	-0.057	0.199	259
G4	-0.227 ± 0.040	-0.102	0.110	125
G5	-0.225 ± 0.060	-0.191	0.196	113

**Figure 6.** The five subsamples in the $[\text{Fe}/\text{H}] - |Z|$ plane.

disk populations according to the Besançon model of the Galaxy (Robin et al. 2003), it is more reasonable to estimate the metallicity gradient among the different groups only for stars with $1 < |Z| < 3$ kpc. Assuming that the variation of $[\text{Fe}/\text{H}]$ with X can be neglected (see discussions in Sect. 3.4), the vertical metallicity gradients can be estimated with a linear fit to the data using the formula $[\text{Fe}/\text{H}] = a|Z| + b$, which usually provides a higher slope than that from the peak of the distribution at each bin. For comparison, we derive such metallicity gradients for five groups, which is given in Table 2. The metallicity gradients for the four groups G2-G5 are similar with a slope of -0.22 , but have decreasing intercepts from 0.02 (G2) to -0.20 (G5). The regression to G1 gives a slope of -0.367 and an intercept of 0.07. A bootstrap method is used to estimate the errors of the slopes by adopting 1000 simulated samples randomly selected from the observed five groups. The results are shown in Fig. 7.

3.4. Vertical versus radial gradients

When we fit linear relations to $[\text{Fe}/\text{H}]$ as a function of $|Z|$, the variation of $[\text{Fe}/\text{H}]$ with X is assumed to be neg-

**Figure 7.** The five groups in the $[\text{Fe}/\text{H}] - |Z|$ plane.

ligible. This may be the case for G2 to G5. Note that G2 to G5 have different X variations: G3 has nearly a fixed X value and G2 has little X variation, while G4 and G5 have significant X variation. Similar slopes in the $[\text{Fe}/\text{H}]$ versus $|Z|$ fits for G2 to G5 indicate that the variation of $[\text{Fe}/\text{H}]$ with X can be disregarded in the $[\text{Fe}/\text{H}]$ versus $|Z|$ fits. This does not mean that there is no radial (hereafter X is referred to as radial) metallicity gradient. Instead, the decreasing intercept (b in Table 2) from G2 to G5 indicates a negative radial gradient and a linear fit to the b versus median X for G2 to G5 gives a slope of -0.013 dex kpc^{-1} . Such a small slope has no significant effect on the $[\text{Fe}/\text{H}]$ versus $|Z|$ fits for our G2 to G5 where X variations are less than 5 kpc.

The small effect of X variation on the vertical metallicity gradient for G2 to G5 can be further confirmed by similar metallicity distributions among these groups with different median X values for similar $|Z|$ ranges of $1 < |Z| < 3$ kpc. For this purpose, we investigate the cumulative distribution function (hereafter CDF) for $[\text{Fe}/\text{H}]$ via the KS test among the five groups. For the two groups in the anti-Galactocenter direction G4 and G5, similar $[\text{Fe}/\text{H}]$ CDFs with a p -value of 0.14 are shown in Fig. 8. This agrees with Katz et al. (2011) where the two directions toward M3 and M5 in the anti-Galactocenter region show similar $[\text{Fe}/\text{H}]$ distributions. Since G4 is located inside of G5, similar $[\text{Fe}/\text{H}]$ CDFs indicate the variation of metallicity with X is not detectable. Similarly, G2 and G3 have similar $|Z|$ distributions with little or no X variation within the group, and a KS test yields a p -value of 0.33 for the $[\text{Fe}/\text{H}]$ CDFs based on stars with $1 < |Z| < 3$ kpc. Again, G2 is located inside of G3 and similar CDFs indicate X differences between G2 and G3

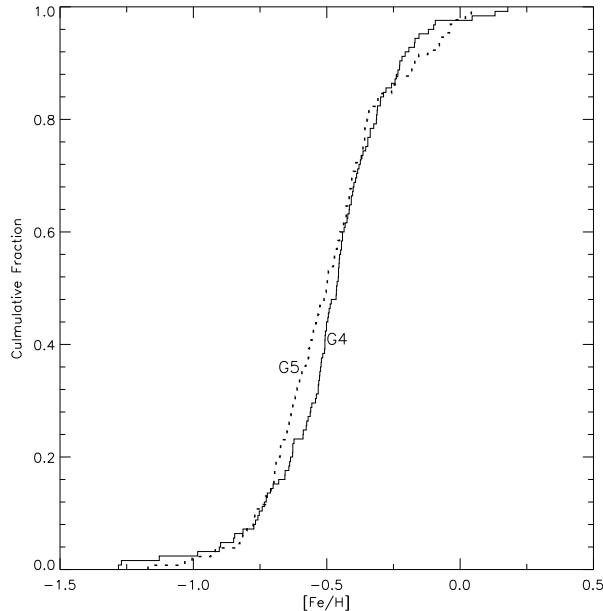


Figure 8. The cumulative distributions of G4 and G5 by KS test.

do not have a significant effect on their metallicity distributions. Similar $[\text{Fe}/\text{H}]$ CDFs are found for G3 and G4, but this is not the case for the comparison between G1 and G5. Fig. 9 shows the similar $|Z|$ but different $[\text{Fe}/\text{H}]$ CDFs between G1 and G5, being the two extreme cases in opposite X directions. For $-0.7 < [\text{Fe}/\text{H}] < -0.4$, G1 and G5 have exactly the same CDFs while at both ends the differences in the $[\text{Fe}/\text{H}]$ CDFs are significant. Two possible reasons may explain the special case of G1. It has been suggested that the effect of $[\text{Fe}/\text{H}]$ variation with X cannot be neglected for a scale length of the thick disk between 2 and 4 kpc. Alternatively, it is expected that G1 has a high contribution of stars at both the metal poor end and the metal rich end from the bulge population with a wide metallicity range of $-2.0 < [\text{Fe}/\text{H}] < 0.5$, which will steepen the gradient. In addition, it seems that G1 also has a special kinematic distribution in Fig. 10, which shows the radial velocity distributions for five groups with G1 having the largest radial velocity range and a peak significantly different from the other groups. Therefore, G1 is not included in this study.

4. SUMMARY

We have estimated the metallicity gradient for the thick disk population in two ways using RHB stars selected from SDSS DR8 data. The first method is based on the Gaussian peak of the metallicity distribution in five $|Z|$ bins by subtracting the contribution from the thin disk and halo via the Besançon Galaxy model. The slope is $-0.12 \pm 0.01 \text{ dex kpc}^{-1}$ with an intercept of -0.34 dex . The second method is linearly fitting the data in the $[\text{Fe}/\text{H}] - |Z|$ diagrams directly for stars from $1 < |Z| < 3 \text{ kpc}$, where the contribution from the thin disk and halo is not significant. Five groups in different directions can be separated to test for consistency, and we found that they give similar gradients of around $-0.225 \pm 0.07 \text{ dex kpc}^{-1}$

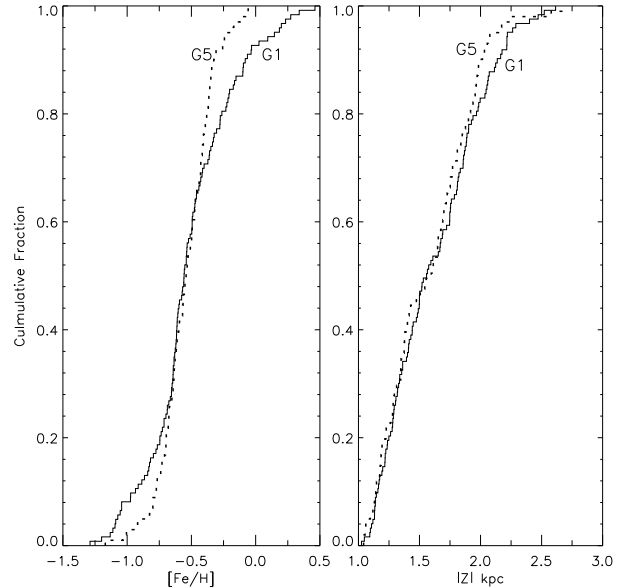


Figure 9. Comparison of the $[\text{Fe}/\text{H}]$ distribution between G1 and G5 by KS test for $1 < |Z| < 3 \text{ kpc}$.

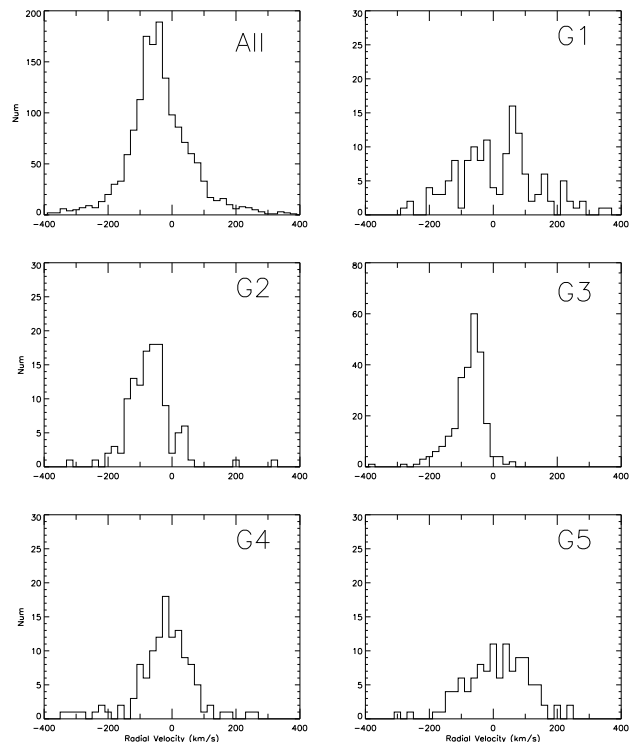


Figure 10. Comparison of the radial velocity distribution for five groups at $1 < |Z| < 3 \text{ kpc}$.

in four groups, with the only exception for the direction with $-4 < X < 4$. Both methods indicate the existence of a metallicity gradient in the thick disk. In our opinion, the first method gives a lower gradient because the model predictions suppress the existence of both metal rich and

metal poor components in the thick disk. We therefore favor the second method with a steeper gradient because it comes from the data directly and thus does not depend on the model assumptions.

This work has been supported by the National Natural Science Foundation of China under grants No. 11073026, 10673015, 10821061, 11078019, the National Basic Research Program of China (973 program) No. 2007CB815103/815403.

Funding for SDSS-III has been provided by the Alfred P. Sloan Foundation, the Participating Institutions, the National Science Foundation, and the U.S. Department of Energy Office of Science. The SDSS-III web site is <http://www.sdss3.org/>. SDSS-III is managed by the Astrophysical Research Consortium for the Participating Institutions of the SDSS-III Collaboration including the University of Arizona, the Brazilian Participation Group, Brookhaven National Laboratory, University of Cambridge, University of Florida, the French Participation Group, the German Participation Group, the Instituto de Astrofísica de Canarias, the Michigan State/Notre Dame/JINA Participation Group, Johns Hopkins University, Lawrence Berkeley National Laboratory, Max Planck Institute for Astrophysics, New Mexico State University, New York University, Ohio State University, Pennsylvania State University, University of Portsmouth, Princeton University, the Spanish Participation Group, University of Tokyo, University of Utah, Vanderbilt Uni-

versity, University of Virginia, University of Washington, and Yale University.

REFERENCES

- Abazajian, K. N., Adelman-McCarthy, J. K., Agüeros, M. A., Allam, S. S., Allende Prieto, C. et al. 2009, *ApJS*, 182, 543
 Aihara H., Allende Prieto, C., An D. et al. 2011, *ApJS*, 193, 29
 Allende Prieto, C., Beers, T. C., Wilhelm, R., Newberg, H. J., Rockosi, C. M., Yanny, B., & Lee, Y. S. 2006, *ApJ*, 636, 804
 Bond, N. A. et al. 2010, *ApJ*, 718, 1
 Carollo, D. et al. 2010, *ApJ*, 712, 692
 Chen, Y. Q., Zhao G., & Zhao J. K. 2009, *ApJ*, 702, 1336
 Chen, Y. Q., Zhao, G., Zhao, J. K. et al. 2010, *AJ*, 140, 500
 Gilmore, G. & Reid, N. 1983, *MNRAS*, 202, 1025
 Ivezić, Ž., Sesar, B., Jurić, M., Bond, N., & Dalcanton, J. 2008, *ApJ*, 684, 287
 Juric, M., Ivezić, Ž., Brooks, A., Lupton, R. H., Schlegel, D. et al. 2008, *ApJ*, 305, 125
 Katz D., Soubiran C., Cayrel R. et al. 2011, *A&A*, 525, A90
 Maciel, W. J. & Costa, R. D. D. 2009, *IAUS Symp.* 256, ed. Cunha K., Spite M., & Barbuy B. (astro-ph/0911.3763)
 Majewski, S. R. 1994, in *Astronomy from wide-field imaging: proceedings of IAU Symp.* 161, ed. H.T. McGillivray, E.B. Thomson, B.M. Lasker, I.N. Reid, D.F. Malin, R.M. West & H. Lorenz (Dordrecht: Kluwer), 425
 Morrison, H. L., Flynn, C., & Freeman, K. C. 1990, *AJ*, 100, 1191
 Robin, A. C., Haywood, M., Creeze, M., Ojha, D. K., & Bienaymé, O. 1996, *A&A*, 673, 864
 Robin A. C., Reylé C., Derrière S., & Picaud S. 2003, *A&A*, 409, 523
 Siegel M. H., Karatas Y., & Reid I. N. 2009, *MNRAS*, 395, 1569
 Soubiran, C., Bienaymé, O., & Siebert, A. 2003, *A&A*, 398, 141
 Yanny B., Rockosi C., Newberg H. et al. 2009, *AJ*, 137, 4377